Available online at www.sciencedirect.com
ScienceDirect
Journal of Hazardous Materials 151 (2008) 380–388
Journal of Hazardous Materials
www.elsevier.com/locate/jhazmat

Adsorptive features of chitosan entrapped in polyacrylamide hydrogel for Pb^{2+}, UO_2^{2+}, and Th^{4+}

Recep Akkaya, Ulvi Ulusoy *

Cumhuriyet University, Department of Chemistry, Sivas 58140, Turkey

Received 9 January 2007; received in revised form 29 May 2007; accepted 31 May 2007
Available online 3 June 2007

Abstract

Chitosan (Ch) was entrapped in polyacrylamide (PAA) by direct polymerization of acrylamide in a suspension of Ch. The adsorptive features of PAA–Ch and Ch were then investigated for Pb^{2+}, UO_2^{2+}, and Th^{4+} in view of dependency on ion concentration, temperature, and kinetics. Additional considerations were also given to their ion selectivity and reusability.

Isotherms were L and H type of Giles classification and evaluated with reference to Langmuir, Freundlich, and Dubinin–Radushkevich (DR) models. PAA–Ch had higher adsorption capacity than Ch for all studied ions so that the sequences were $Th^{4+} > Pb^{2+} > UO_2^{2+}$ concordantly with their affective ionic charges. The affinity of Ch in PAA increased for Pb^{2+} and UO_2^{2+} but did not change for Th^{4+}.

The values of enthalpy and entropy changed were positive for all studied ions for both Ch and PAA–Ch. The negative free enthalpy change value indicated that the adsorption process is spontaneous in the sequence of $Th^{4+} \geq Pb^{2+} > UO_2^{2+}$. Free energy values derived from DR model implied that the sorption process is the ion exchange. Well compatibility of adsorption kinetics to the pseudosecond-order model predicate that the rate-controlling step is a chemical sorption.

The study for ion selectivity showed that both Ch and PAA–Ch had the highest affinity to Pb^{2+}. The reusability tests for Ch and PAA–Ch for Pb^{2+} for five uses showed that complete recovery of the ion was possible.

The studied features of PAA–Ch suggest that the material should be considered as a new adsorbent. It is envisaged that the use of Ch in PAA will enhance practicality and effectiveness of Ch in separation and removal procedures.

Keywords: Chitosan; Composite; Metal; Adsorption; Polyacrylamide

1. Introduction

The metal (radioactive or not) ions, contributed into nature by natural or industrial resources, are of environmental concerns due to their possible detrimental affects associated with radioactivity and/or toxicity to the biological systems, even they are present at trace levels. Therefore, remediation for wastewater becomes necessary and corresponding techniques are needed. Besides this, the recovery of some metals may also be of economical interests. Flotation, coagulation, precipitation, extraction, ion exchange, and electrolytic procedures are conventionally applied methods. However, excessive time requirements, high costs, and production of highly toxic sludge are the constraints of these techniques [1,2].

The adsorption procedures are introduced as a favorable way for the remediation processes, because of its efficacy, practicality, and economical feasibility, depending on the used adsorbents. The adsorbents possessing lower cost are very abundant in the nature [3,4]. Chitosan (Ch) is *N*-deacetylated derivative of chitin [poly-β-(1→4) linked *N*-acetylglucosamine] which is one of the commonly used adsorbents, since chitin is the second most abundant compound in the nature after cellulose [5], besides its antimicrobial, antibacterial, antifungal, and biodegradable features [6].

* Corresponding author. Tel.: +90 346 2191010x1623; fax: +90 346 2191186.
E-mail address: ulusoy@cumhuriyet.edu.tr (U. Ulusoy).

0304-3894/$ – see front matter © 2007 Elsevier B.V. All rights reserved.
doi:10.1016/j.jhazmat.2007.05.084

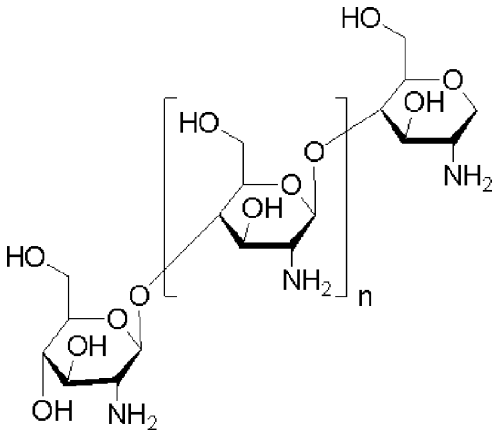

In fact, recent applications coherently show the advantages of chitosan (with or without modifications) in the removal of metal ions. For example, Simionato et al. [7] used chitosan obtained from silkworm chrysalides for the removal of Al^{3+} from textile water. Cr^{6+} and Cu^{2+} adsorption onto chitosan with particular attention to the kinetics were studied by Sag and Aktay [8]. Gyliene et al. [9] investigated sorption capability of chitosan for Cu^{2+}-EDTA and its regeneration by electrolysis. Co^{2+} was of interest together with copper, where crap shell particles was the adsorbent [10]. Fe^{2+} and Fe^{3+} sorption characteristics of chitosan and its cross-linked form were differentiated by Ngah et al. [11]. Chitosan modified to amine and azole resins were investigated for sorption of Hg^{2+} and $UO_2{}^{2+}$ by Atia [2], chitosan microspheres cross-linked with tripolyphosphate was used for the removal of both acidity and Fe^{3+} and Mn^{2+} in contaminated water in coal mining [12]. Cross-linked carboxymethyl-chitosan with Pb^{2+} as template ions was the adsorbent for lead removal in the study reported by Sun et al. [13] and Th^{4+} imprinted chitosan-phytalate particles was used for selective sorption of thorium by Birlik et al. [14].

Further researches require enhancing practical usage of chitosan since it has some usage limitations due to its nonporosity, low surface area, and particularly the unsuitable particle characteristics resulting in hydrodynamic limitations and column fouling [4]. One possible solution to these limitations can be to embody chitosan into an inert media. This media should be capable of swelling (hydrophilic) in aquatic solutions, enabling the diffusion and/or transfer of ions towards chitosan. A hydrogel polymer for example, cross-linked polyacrylamide (PAA) should provide these requirements. Indeed, it was proved that the immense improvements in the adsorptive features of bare clay or zeolite were obtainable, when an adsorptive mineral was dispersed in PAA as the other component of the composite [15].

In this work, the composite of chitosan (Ch) with PAA was introduced as a new material (PAA–Ch) to provide practical use of Ch. The preparation and characterization of PAA–Ch, and its comparative adsorptive features with pure Ch with reference to the dependency on concentrations and temperature, and the adsorption kinetics for lead, uranium, and thorium ions (Pb^{2+}, $UO_2{}^{2+}$, and Th^{4+}) were investigated. The metal cations represented the hazardousness in view of toxicity and radioactivity, different oxidation states, and ionic compositions in addition to chemical similarities of Th and the rare earth ions [16]. The adsorptive features were evaluated on the basis of adsorption parameters derived from the compatibility of adsorption isotherms to the Langmuir, Freundlich, and Dubinin–Radushkevich (DR) models. Additional considerations were also given to the ion selectivity and reusability of the composite for the studied ions.

2. Experimental

2.1. Reagents

Acrylamide monomer, N,N′-methylenebisacrylamid, N,N,N′,N′-tetramethylethylenediamine, chitosan from crab shells [poly-(1,4-β-D-glucopyranosamine)], $Pb(NO_3)_2$, $UO_2(NO_3)_2 \cdot 6H_2O$, and $Th(NO_3)_4 \cdot 4H_2O$ were purchased from SigmaAldrich. Arsenazo III (disodium salt) was obtained from Acros. Merck was the supplier of 4-(2′-pyridylazo)-resorcinol (PAR). All chemicals used were of analytical reagent grade. No pretreatment was applied to the reagents.

All experiments were always performed in duplicates. The limit of experimental error of each duplicate was ±5%, any experiment resulting in higher than this limit was repeated.

2.2. Preparation of PAA–Ch

For preparation of 3 g of PAA–Ch, 1 g of Ch in 20 mL of water was stirred 15 min to obtain a homogeneous suspension. Ten milliliters of solution containing 2 g of acrylamide monomer to provide a mass ratio 2:1 was added to the suspension and stirred for an additional 5 min. 0.2 g of N,N′-methylenebisacrylamide and 50 mg ammoniumpersulphate dissolved in 10 mL distilled water was contained onto the suspension. Finally, 100 μL of N,N,N′,N′-tetramethylethylenediamine was added to propagate the polymerization at 25 °C [17]. PAA–Ch gel was washed after completion of the polymerization with distilled water until the effluent attained neutral pH. The gel was dried at ambient temperature, ground, and sieved to a particle −25 mesh size, and stored in polypropylene container. To avoid the variations in characteristics dependent on the preparation, a 50 g lot of PAA–Ch was prepared to conduct the overall investigation.

FT–IR spectrometric (Mattson 1000, UK) analysis was used to characterize the chemical structure of Ch and PAA–Ch. All samples were prepared as KBr pellets and spectra were taken at a resolution of 4 cm^{-1}. Adsorption surface area and porosity of the adsorbents were also determined by the use of N_2 sorption system (Quantachrome Instruments).

Pure PAA was also prepared for comparison of swelling features of the composite and Ch with PAA. The water imbibing feature of PAA–Ch was also tested in the presence of the studied ions to reveal if there was any effect of ionic strength on the swelling. Dried samples of 0.1 g each were weighed and let to swell in tubes for the equilibrium with water and the solutions of studied ions (250, 500, 1000, and 2000 ppm), the swollen samples were then weighed to find swelling ratio as percentage with reference to the dry weights.

2.3. Pb^{2+}, UO_2^{2+}, and Th^{4+} adsorption

Adsorptive features of the adsorbents were investigated for Pb^{2+}, UO_2^{2+}, and Th^{4+}. 0.1 g of Ch and PAA–Ch in the studied solutions was equilibrated with 10 mL of Pb^{2+}, UO_2^{2+}, and Th^{4+} at concentrations within the range of 1×10^{-4} to 8×10^{-3} mol L^{-1} (25–2000 ppm). The adsorbent–solution systems were equilibrated for 24 h at 298 K in a thermostatic water bath and the suspensions were then centrifuged at 2500 rpm for 5 min. The initial/final pH values of the solutions were 4.5/5 for Pb^{2+}, 3.1/5 for UO_2^{2+}, and 3.5/5 for Th^{4+}, which were below the precipitation pH of the ions at studied concentrations. Mass dependency of the adsorption was also checked for Ch and PAA–Ch. Duplicates of 25, 50, 75, and 100 mg of Ch and PAA–Ch were interacted with solutions of the ions at 5×10^{-3} mol L^{-1} by following the procedure given above.

The metal-dye detection procedure provided by Laussmann et al. [18] was modified for Pb^{2+} determination in the supernatants. A solution of 3.5×10^{-3} mol L^{-1} of PAR in 0.7 mol L^{-1} of Tris–HCl at pH 8–9 was prepared. A 50 μL fraction of supernatant was added onto 3 mL of the reagent and the absorbance of the formed metal complex was measured at 510 nm. Arsenazo III was used as the dying reagent in the determination of UO_2^{2+} and Th^{4+} [19,20]. The solutions containing 0.04% Arsenazo III in HCl to provide pH 1.5 for UO_2^{2+} and in 2 M $HClO_4$ for Th^{4+} analysis were prepared. A 50 μL fraction of supernatant was added onto 3 mL of the reagent and the absorbance was measured at 650 nm.

To confirm accuracy of the results obtained from the metal-dye detection, UO_2^{2+} and Pb^{2+} in some selected samples were also determined by radioactivity measurements by means of a gamma spectrometer [NAI(Tl) detector combined with a EG and G ORTEC multichannel analyzer and software, MAESTRO 32, MCA Emulator, USA was employed]. ^{212}Pb at secular equilibrium with ^{232}Th isolated from Th was used as isotopic tracer to monitor Pb^{2+} adsorption. The activity is measured at 186 keV of ^{235}U at natural level in uranium composition and that at 238.6 keV of ^{212}Pb.

2.4. Temperature dependence of Pb^{2+}, UO_2^{2+}, and Th^{4+} adsorption

Temperature effect on adsorption for determination of thermodynamic parameters was studied for three temperatures: 283, 298, and 313 K. Duplicates (0.1 g each) of Ch and PAA–Ch were equilibrated with solutions of Pb^{2+}, UO_2^{2+}, and Th^{4+} at 3×10^{-3} mol L^{-1} at the chosen temperatures for 24 h. The samples were subjected to the same procedure described above; equilibrium concentrations and adsorbed amounts were determined.

2.5. Adsorption kinetics

Ten milliliters of solution of each ion was added on to 0.1 g of Ch and PAA–Ch as duplicates. Fifty-microliter fractions of solution were withdrawn for 4 h, starting immediately after the solution–solid contact and continued with time intervals. Pb^{2+}, UO_2^{2+} and Th^{4+} contents of the fractions were determined as described above. A correction factor was applied to data by considering the volume decrease in equilibrium solutions due to sampling.

2.6. Ion selectivity and reusability

The ion selectivity of Ch and PAA–Ch from solutions containing possible combinations of studied ions at equivalent concentrations (5×10^{-3} mol L^{-1}) was studied. Ten-milliliter fraction of solutions containing the ions at possible combinations were poured on 0.1 g (duplicates) of Ch and PAA–Ch, the ion contents of equilibrium (after 24 h) solutions were measured. Neither Th^{4+} and Pb^{2+} nor UO_2^{2+} had any interference with each other when Th^{4+} was determined with Arsenazo III in 2 mol L^{-1} of $HClO_4$ [19,20]. Gamma spectrometric method was employed for the determination of Pb^{2+} and UO_2^{2+}.

Hydrochloric acid at 0.5–1 mol L^{-1} is known as an effective regenerator for resins [21,22]. This effluent was also tested for Ch and PAA–Ch with a reusability study for Pb^{2+}. To accomplish this, five duplicates of 0.1 g Ch and PAA–Ch in polypropylene tubes were equilibrated with 10 mL of 4×10^{-3} mol L^{-1} Pb^{2+} for 24 h and the adsorbed amounts were derived from the ion contents of supernatants. The contents of columns were eluted with 5 mL fractions of 15 mL of 1 mol L^{-1} HCl and the columns were then washed with distilled water until the effluents had a neutral pH. The Pb^{2+} contents of the effluents (HCl) were determined. Each sample was subjected to the same procedure for four sequential times to provide five uses in total.

2.7. Data evaluation

The amounts of adsorption of the ions of interest (Q, mol kg^{-1}) were calculated from $Q = [(C_i - C_e)V/w)]$, where C_i and C_e are the initial and equilibrium concentrations (mol L^{-1}), w is the mass of adsorbent (kg) and V is the solution volume (L). The Langmuir [$Q = (K_L X_L C_e)/(1 + K_L C_e)$] and Freundlich ($Q = X_F C_e^{1/\beta}$) models were fit to the isotherms experimentally obtained, where X_L is the monolayer sorption capacity (mol kg^{-1}) and K_L is the adsorption equilibrium constant (L mol^{-1}) related to the adsorption energy. X_F and '$1/\beta$' are empirical Freundlich constants associated with the capacity and intensity of adsorption ($1/\beta$ represents the heterogeneity of the adsorptive surface). The isotherms were also evaluated with reference to Dubinin–Radushkevich model to find out the constant (K_{DR}; mol^2 K J^{-2}) related to the sorption energy from $Q = X_{DR} e^{-K_{DR}\varepsilon^2}$, where X_{DR} is sorption capacity (mol kg^{-1}) and $\varepsilon = RT \ln(1 + 1/C_e)$ is Polanyi potential. Free energy change (E; J mol^{-1}) required to transfer one mole of ion from the infinity in the solution to the solid surface was derived from $E = (-2K_{DR})^{1/2}$ [23,24].

The thermodynamic parameters were determined as follows: the distribution coefficients (K_d) were derived from $K_d = Q/C_e$

for each temperature and '$\ln K_d$' was depicted against $1/T$ to provide adsorption enthalpy (ΔH, J mol^{-1}) and entropy (ΔS, J mol^{-1} K^{-1}) from the slopes ($\Delta H/R$) and intercepts ($\Delta S/R$) of the depictions with reference to '$\ln K_d = [(\Delta S/R) - (\Delta H/R)1/T]$', where R is ideal gas constant, 8.314 J mol^{-1} K^{-1}, and T is the absolute temperature. Having had ΔH and ΔS, ΔG values were calculated from $\Delta G = \Delta H - T\Delta S$ for 298 K.

Pseudosecond-order kinetic and intraparticle diffusion rate equations were applied to the results of kinetic studies to be able to envisage the controlling mechanism of the adsorption process. $t/Q_t = 1/(kQ_e^2) + t/Q_e$ and $Q_t = k_i t^{1/2}$ (Weber and Morris model), where Q_t and Q_e are the adsorption capacities (mol kg^{-1}) at time t and equilibrium, k and k_i are the rate constants. Initial adsorption rate was also calculated from $h = kQ_e^2$ [25,26].

A t-test was applied to obtain the significance of regression coefficients (R^2) for the compatibility of experimental data to the Langmuir, Freundlich and DR models, and for those to the linearity of kinetic equations; $p < 0.01$ was considered as the threshold for the significance [27].

3. Results and discussion

3.1. Structural evaluation

The FT–IR spectra of Ch and PAA–Ch were compared in Fig. 1(a) and (b). Broad band of O–H and N–H of 3200–3500 cm^{-1} sharpened and intensified in PAA–Ch, which was associated with the intramolecularly H-bonded terminals in Ch that was unbridged and became strengthened when embodied in PAA. Similar explanation was also possible for the change in vibrations around 3100 and 1650 cm^{-1} of N–H. The sharp peak at 1680 cm^{-1} of C=O was evidence for the involvement of PAA into the composition. The counters within the range 1320–1500 cm^{-1} were of associates N–H of amine and amide of PAA, whilst the band at around 100–1140 cm^{-1} was of cyclic ether of Ch, C–O–C [13,14,28].

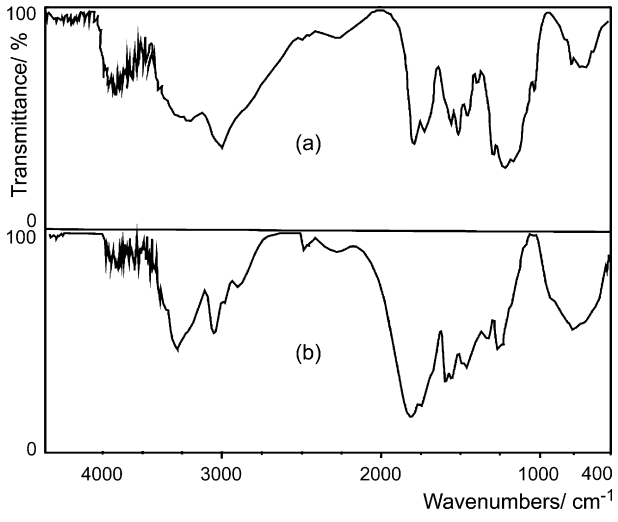

Fig. 1. FT–IR spectra of Ch (a) and PAA–Ch (b).

Table 1
Physical characteristics of Ch and PAA–Ch

	Ch	PAA–Ch
Multipoint BET surface area (m^2 g^{-1})	1.43	2.02
Pore volume (cm^3 g^{-1})	0.010	0.008
Pore diameter (nm)	3.0	2.7

The results of adsorption surface area and porosity measurements were provided in Table 1. Both adsorbents had mesoporosity with reference to the IUPAC classification, since their pore diameter values are within the range of 2–50 nm. The pore size and pore volume of the materials were not significantly different from each other, but PAA–Ch had a wider BET surface area than Ch.

With the increase in number of hydrophilic terminals, the water imbibing feature (hydrogel) of PAA–Ch increased in comparison with those of its components individually, so that the magnitude of swelling were found to be 1200% for Ch, 1350% for PAA and 1600% for PAA–Ch. The mean value of swelling in solution containing the studied ions was found to be 1500%. This was slightly lower than its magnitude in water, but there was not any systematic relation between the ionic strength of the medium and the swelling for the studied concentration range. Since the adsorption was calculated on the basis of dry weights of adsorbents, slight shrink in swelling of PAA–Ch was not considered as an effective parameter.

3.2. Pb^{2+}, UO_2^{2+}, and Th^{4+} adsorption

Experimentally attained adsorption isotherms and their compatibility to Langmuir and Freundlich models of Pb^{2+}, UO_2^{2+}, and Th^{4+} were provided in Fig. 2. The parameters derived from the models, including DR (not figured), were contained in Table 2. The adsorption capacities derived from the studied models (X_L, X_F, and X_{DR}) were concordantly in the order of $Th^{4+} > Pb^{2+} > UO_2^{2+}$ for both Ch and PAA–Ch, but the values increased significantly in favor of PAA–Ch (see the expected adsorptions derived from X_L given under brackets in Table 2 and Fig. 3). This can be attributed to PAA in PAA–Ch. The Ch dispersed in the hydrogel finely, resembling a colloidal behavior of one solid phase Ch in another PAA, which causes an expansion of the adsorptive surface and minimizes possible cause of steric hindrance to adsorption due to inter/intra molecularly interacted active sites of Ch.

The sequence of K_L values, as a measure of spontaneity of adsorption, was $Pb^{2+} > UO_2^{2+} > Th^{4+}$ and agree with the trend seen in 'β' as a measure of increasing surface heterogeneity of Freundlich [2,7]. The values of 'β' and 'K_L' justified each other for Pb^{2+} and UO_2^{2+}, indicating that the higher amount adsorbed is the ion with the higher tendency to be adsorbed onto the adsorbent. This was not valid for Th^{4+}, for which K_L as well as 'β' was smallest, whilst the capacity (X) was the highest. This should be associated with the affective ionic charge (radii/ionic charge) which is in the sequence of UO_2^{2+} (253 pm/2) > Pb^{2+} (119 pm/2) > Th^{4+} (94 pm/4) [16], the smaller has the higher

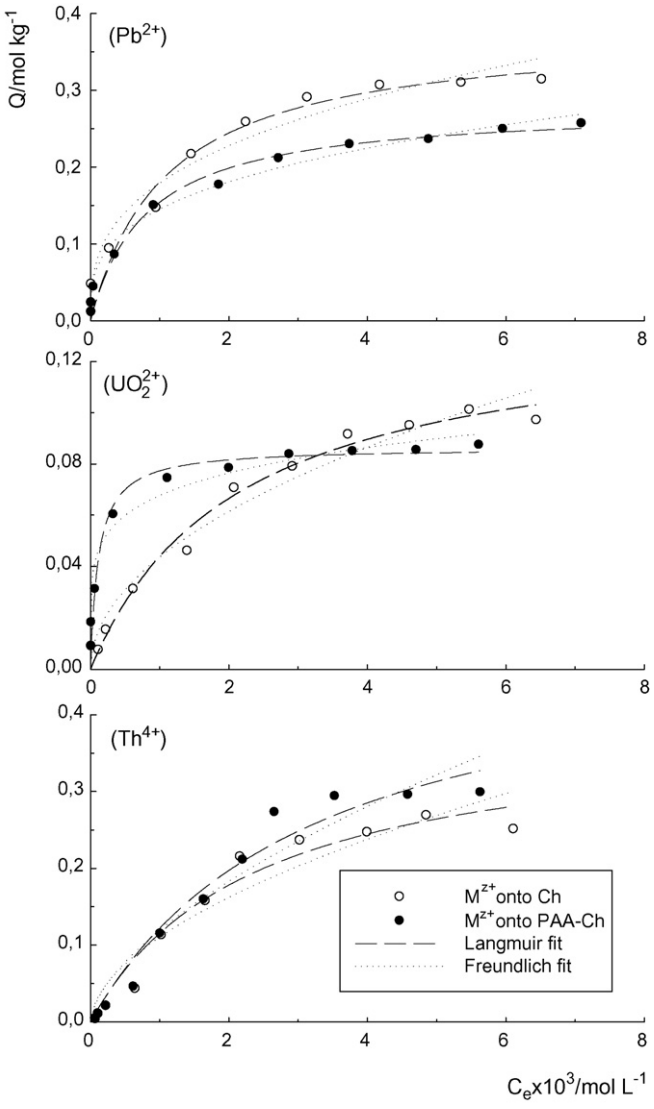

Fig. 2. Experimentally obtained adsorption isotherms Pb^{2+}, $UO_2{}^{2+}$, and Th^{4+}, and their compatibility to Langmuir and Freundlich models.

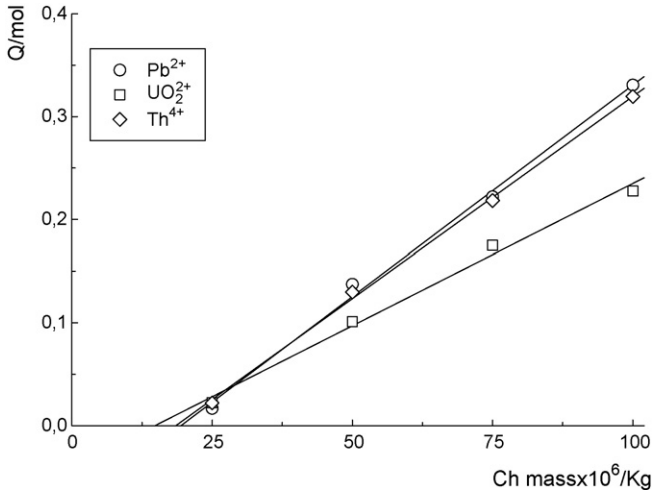

Fig. 3. Adsorption dependence of the studied ions to Ch mass (values of R^2 are 0.995 for Pb^{2+}, 0.996 for $UO_2{}^{2+}$, and 0.998 for Th^{4+}).

mobility in the solution and in the hydrogel, for which the required energy for migration of ions towards the adsorbent and transference to the active sites to form complex expected to be lower than the others. Active terminals ($-NH_2$ groups) of Ch were attracted towards the metal species to form complex by ion exchange with two possible ways: by chelation (bridge model) of an ion with multiple coordination with inter and/or intramolecular amine terminals and by pendant coordination of an ion with an amine terminal [29]. The former is expected to be more stable, but requires steric convenience and more numbers of active terminals than the latter. In any case, the conditions seem to be in favor of Th^{4+} ions. However, the highest decrease in adsorption due to PAA involvement was for $UO_2{}^{2+}$ ions, implying the ion with the highest ratio has the least capability to pass through the PAA network and to make complex with the sites.

3.3. Adsorption thermodynamics

Temperature dependence of the adsorption of the studied ions were shown in Fig. 4, '$1/T$' as a function of '$\ln K_d$', from which

Table 2
Langmuir, Freundlich, and Dubinin–Radushkevich parameters for Pb^{2+}, $UO_2{}^{2+}$, and Th^{4+} onto Ch and PAA–Ch

	Langmuir			Freundlich			DR	
	X_L ($mol^{-1}\,kg^{-1}$)	K_L ($L\,mol^{-1}$)	r^2	X_F	β	r^2	X_{DR}	r^2
Pb^{2+}								
Ch	0.38	914	0.969	1.94	2.9	0.956	0.85	0.969
PAA–Ch	0.28 (0.84)[a]	1236	0.975	1.27	3.2	0.982	0.46	0.980
$UO_2{}^{2+}$								
Ch	0.14	472	0.984	1.32	2.2	0.964	0.36	0.991
PAA–Ch	0.09 (0.27)	8569	0.941	0.23	5.5	0.926	0.14	0.962
Th^{4+}								
Ch	0.39	422	0.966	5.01	1.8	0.920	2.4	0.978
PAA–Ch	0.51 (1.53)	312	0.968	8.39	1.6	0.935	2.6	0.981

[a] Expected X_L with reference to the composite containing 0.1 g of Ch (mass ratio of Ch/PAA–Ch for the composite was 1/3 and the adsorbed amount was linearly proportional with Ch mass, see Fig. 3).

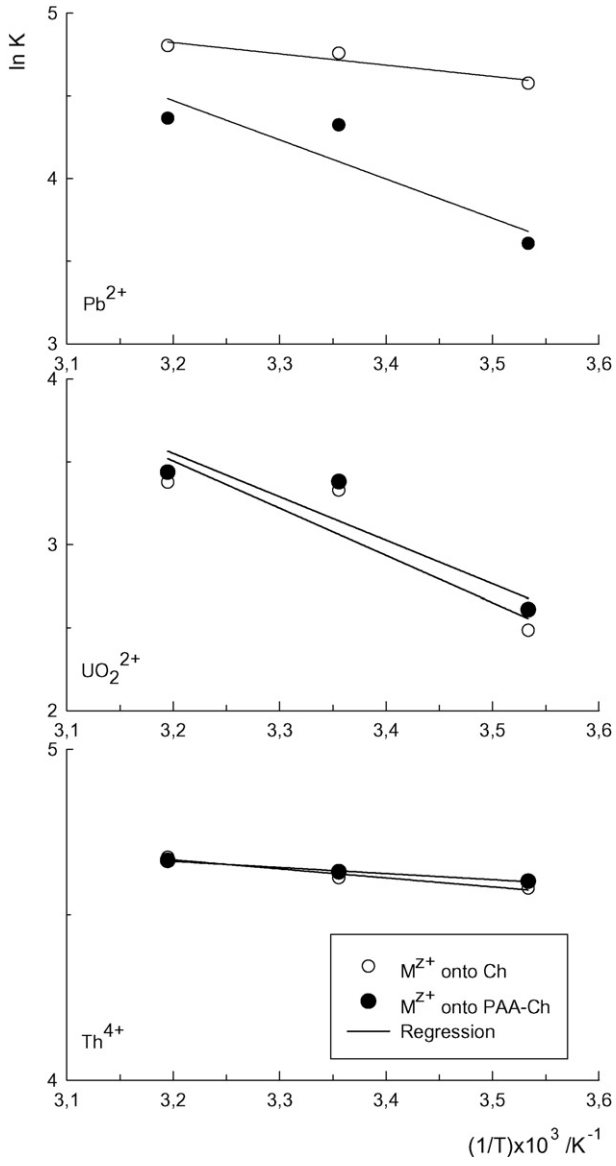

Fig. 4. Temperature dependence of the adsorption for studied ions.

the thermodynamic parameters were obtained and submitted in Table 3. Constant related to sorption energy (K_{DR}) and free energy change (E_{DR}) derived from DR model were also provided in the table.

The enthalpy changed for the adsorption was $\Delta H > 0$ for all ions for both Ch and PAA–Ch, indicating that the overall process was endothermic and, the order of ΔH values was $UO_2^{2+} > Pb^{2+} > Th^{4+}$ showing a similar trend with the K_{DR}. The values of entropy changed were positive for all ions for both adsorbents showing that the randomness in the solid–solution interface increased along with the adsorption process. Gibbs free enthalpy change was $\Delta G < 0$ indicating that the adsorption process is spontaneous in the sequence of $Th^{4+} \geq Pb^{2+} > UO_2^{2+}$. $E_{DR} \cong 8\,kJ\,mol^{-1}$ has been assumed as a threshold for definition of the nature of adsorption; the physical forces such as diffusion process are effective on sorption if $E_{DR} < 8\,kJ\,mol^{-1}$, the nature of process is chemical (the complex formation/ion exchange) otherwise [23,29]. The E_{DR} values imply that the process was chemical sorption.

3.4. Kinetics of adsorption

The first-order kinetics describes a reversible equilibrium established between the ions in solution and those adsorbed on solid phase, whereas the second-order model defines that the rate-controlling mechanism is chemical process [11,25].

The compatibility of the adsorption kinetics of the studied ion on to Ch and PAA–Ch to the second-order equation (t/Q_t *versus* t) was provided in Fig. 5. The figure also contained the plots of Q_t *versus* $t^{0.5}$ from which intraparticle diffusion rates were obtained. The parameters derived from the figures were presented in Table 4.

The well compatibility to the second order kinetics indicated that the process was ion concentration dependent so that the rate-controlling step is chemical sorption via complex formation/ion exchange. The plot of Q_t *versus* $t^{0.5}$ (Weber and Morris model) showed that two types of mechanisms take place in the adsorption process; the initial rapid uptake under the boundary layer effects and the slow intraparticle diffusion after the completion of external coverage [30]. Intraparticle diffusions rate constant were obtained from the slopes of the latter's trends. The found diffusion rate constants for PAA–Ch were higher than those of Ch for all ions. This should also be associated with the fine dispersion of Ch in PAA enabling Ch expansion of adsorptive surface so that the probability of transference of the ions towards the inner active sites increased.

Table 3
Thermodynamic parameters for Pb^{2+}, UO_2^{2+}, and Th^{4+} adsorption onto Ch and PAA–Ch

	ΔH (kJ mol^{-1})	ΔS (J mol^{-1} K^{-1})	ΔG (kJ mol^{-1})	$-K_{DR}$ ($\times 10^9$ mol^2 K J^{-2})	E_{DR} (kJ mol^{-1})
Pb^{2+}					
Ch	5.7	58	−11.6	5.4	9.6
PAA–Ch	19.7	101	−10.4	3.8	11.5
UO_2^{2+}					
Ch	23.7	105	−7.6	7.3	8.3
PAA–Ch	21.8	100	−8.0	2.4	14.5
Th^{4+}					
Ch	2.3	46	−11.4	10.8	6.8
PAA–Ch	1.5	44	−11.6	10.8	6.8

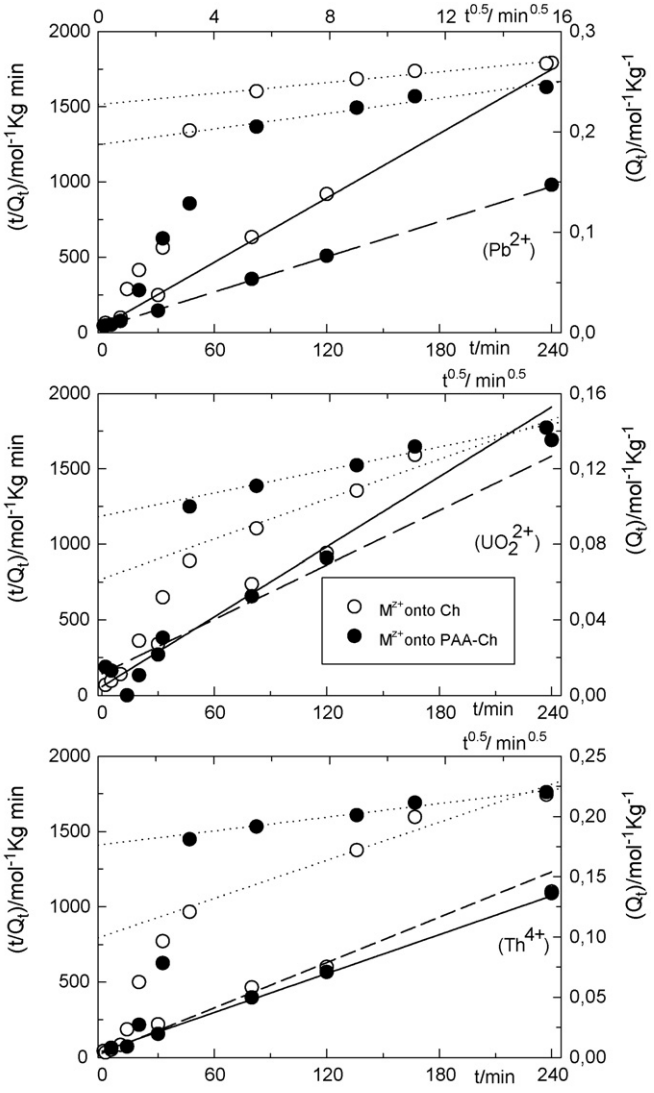

Fig. 5. Compatibility of Pb^{2+}, $UO_2{}^{2+}$, and Th^{4+} adsorption kinetics for Ch and PAA–Ch to pseudosecond-order model (plots t/Q_t *vs.* t with solid and short dashed lines) and to Weber–Morris model (plots Q_t *vs.* $t^{0.5}$ with dotted lines).

Table 5
Ion selectivity of Ch and PAA–Ch from solutions containing possible combinations of studied ions at equivalent concentrations (5×10^{-3} mol L^{-1})

Ion combinations	Adsorption (%)	
	Ch	PAA–Ch
Pb^{2+}, $UO_2{}^{2+}$, and Th^{4+}		
Pb^{2+}	95[a] (55)[b]	95 (57)
$UO_2{}^{2+}$	39 (23)	37 (22)
Th^{4+}	37 (22)	35 (21)
Pb^{2+} and $UO_2{}^{2+}$		
Pb^{2+}	95 (80)	95 (72)
$UO_2{}^{2+}$	23 (20)	36 (28)
Pb^{2+} and Th^{4+}		
Pb^{2+}	32 (55)	38 (51)
Th^{4+}	26 (45)	37 (49)
$UO_2{}^{2+}$ and Th^{4+}		
$UO_2{}^{2+}$	64 (58)	68 (58)
Th^{4+}	47 (42)	50 (42)

[a] As percentage of the amount of ion added to the solution.
[b] As percentage adsorption of total ion adsorption onto the adsorbent.

3.5. Ion selectivity and reusability

Ion selectivity of the adsorbent in the presence of the studied ions with all possible combinations at equivalent concentrations (5×10^{-3} mol L^{-1}) was compared in Table 5.

Both Ch and PAA–Ch had the highest affinity to Pb^{2+} in the presence of both $UO_2{}^{2+}$ and Th^{4+} and of $UO_2{}^{2+}$. This can also be explained by the affects of the affective ionic charge and the parameters related to the affinity of Pb^{2+} to the adsorbents (K_L and β, see Table 2) together with the ionic strength of the medium; it appears that all were in favor of Pb^{2+}. As a result of these factors, similar affinity trends were also observed for the other two possible combinations, for Pb^{2+} from Pb^{2+} and Th^{4+} and for $UO_2{}^{2+}$ from $UO_2{}^{2+}$ and Th^{4+}.

The reusability feature of Ch and PAA–Ch was tested for Pb^{2+} for four regenerations in a total of five uses. Percentage adsorption of the ion onto the adsorbents and the regeneration efficiency for each use was provided in Table 6. The means and its ±S.E.M of the adsorption and the recovery efficiency obtained from the following uses after the first were found to be 50.0 ± 1.5 and 100 ± 2 for Ch and 37.9 ± 1.1 and

Table 4
Kinetic parameters for Pb^{2+}, $UO_2{}^{2+}$, and Th^{4+} adsorption onto Ch and PAA–Ch

	Pseudosecond-order kinetic			Intraparticle diffusion rate	
	K (mol^{-1} kg min^{-1})	H (mol kg^{-1} min)	R^2	K_i ($\times 10^3$ mol kg^{-1} $min^{0.5}$)	R^2
Pb^{2+}					
Ch	0.61	0.05	0.988	3.7	0.999
PAA–Ch	0.41	0.03	0.996	5.5	0.999
$UO_2{}^{2+}$					
Ch	1.04	0.02	0.984	6.1	0.981
PAA–Ch	0.25	0.01	0.958	3.5	0.983
Th^{4+}					
Ch	0.89	0.04	0.958	8.5	0.978
PAA–Ch	0.45	0.02	0.996	3.2	0.978

Table 6
Reusability of Ch and PAA–Ch for adsorption of Pb^{2+}

Reusage no[a]	Adsorption (%)	
	Ch	PAA–Ch
1	49.9	37.9
2	49.5 (99)[b]	37.1 (98)
3	50.8 (102)	41.0 (108)
4	51.9 (104)	38.0 (100)
5	47.9 (96)	35.5 (94)
Mean ± S.D.M.	50.0 ± 1.5 (100 ± 2)	37.9 ± 1.1 (100 ± 3)

[a] Number of sequential usage of the adsorbent.
[b] Regeneration efficiencies with reference to the first use.

100 ± 3 for PAA–Ch. The values of means were not significantly different from the values of their first use and 100% ($p < 0.05$). The IR spectra obtained before and after reuses provided no evidence signifying any changes in the structures. Storage foregoing also had no effect on the structural stability.

4. Conclusion

The preparation and characterization of PAA–Ch, and its comparative adsorptive features with pure Ch with reference to the dependency on concentrations and temperature, and the adsorption kinetics for Pb^{2+}, $UO_2{}^{2+}$, and Th^{4+} were investigated.

Experimentally attained isotherms were L and H type of Giles classification. PAA–Ch had higher adsorption capacity than Ch for all studied ions so that the sequences were $Th^{4+} > Pb^{2+} > UO_2{}^{2+}$ concordantly with their affective ionic charges for both adsorbents. The affinity to Ch in PAA increased for Pb^{2+} and $UO_2{}^{2+}$ but not changed for Th^{4+}.

The values of enthalpy and entropy changed were positive for all ions for both Ch and PAA–Ch. Free energy values derived from DR model and well compatibility of adsorption kinetics to the second order implied that the sorption process is chemical.

Ch and PAA–Ch had the highest affinity to Pb^{2+} in the presence of the other two ions. The regeneration tests for Ch and PAA–Ch showed that both adsorbents can be reused after complete recovery of the loaded ion 1 mol L^{-1} HCl and reconditioned.

As a consequence, the use of Ch in PAA will enhance practicality and effectiveness of Ch in separation and removal procedures.

Acknowledgements

This work was supported by the research fund of Cumhuriyet University (Project No. F-160 granted to Ulvi Ulusoy) to which the authors are grateful. The study is a part of the MSc thesis by Recep Akkaya. The authors also acknowledge P. Hande Oz for BET and porosity analysis in Tubitak-Mam laboratories (Gebze/Turkey).

References

[1] S.J.T. Pollard, G.D. Fowlerr, C.J. Sollars, R. Perry, Low-cost adsorbents for waste and wastewater treatment: a review, Sci. Total Environ. 116 (1992) 31–52.
[2] A.A. Atia, Studies on the interaction of mercury(II) and uranyl(II) with modified chitosan resins, Hydrometallurgy 80 (2005) 13–22.
[3] S. Babel, T.A. Kurniawan, Low-cost adsorbents for heavy metals uptake from contaminated water: a review, J. Hazard. Mater. 3967 (2003) 1–25.
[4] D. Mohan, C.U. Pittman, Activated carbons and low cost adsorbents for remediation of tri- and hexavalent chromium from water, J. Hazard. Mater. 137 (2006) 762–811.
[5] N.Q. Hien, D.V. Phu, N.N. Duy, H.T. Huy, Radiation grafting of acrylic acid onto partially deacetyleted chitin for metal ion adsorbent, Nucl. Instrum. Methods Phys. Res. 236 (2005) 606–610.
[6] X. Wang, Y. Du, J. Yang, X. Wang, X. Shi, Y. Hu, Preparation, characterization and antimicrobial activity of chitosan/layered silicate nanocomposites, Polymer 47 (2006) 6738–6744.
[7] J.I. Simionato, A.T. Paulino, J.C. Garcia, J. Nozaki, Adsorption of aluminium from waste water by chitin and chitosan produced from silkworm chrysalides, Polym. Int. 55 (2006) 1243–1248.
[8] Y. Sag, Y. Aktay, Kinetic studies on sorption of Cr(VI) and Cu(II) ions by chitin, chitosan and *Rhizopus arrhizus*, Biochem. Eng. J. 12 (2002) 143–153.
[9] O. Gyliene, O. Nivinskine, I. Razmute, Copper (II)-EDTA sorption onto chitosan and its regeneration applying electrolysis, J. Hazard. Mater. 137 (2006) 1430–1437.
[10] K. Vijayaraghavan, K. Palanivelu, M. Velan, Biosorption of copper(II) and cobalt(II) from aqueous solutions by crab shell particles, Bioresour. Technol. 97 (2006) 1411–1419.
[11] W.S.W. Ngah, S.A. Ghani, A. Kamari, Adsorption behavior of Fe (II) and Fe(III) ions in aqueous solution on chitosan and cross-linked chitosan beads, Bioresour. Technol. 96 (2005) 443–450.
[12] R. Laus, M.C.M. Laranjeira, A.O. Martins, V.T. Favere, Chitosan microspheres crosslinked with tripolyphosphate used for the removal of the acidity, iron (III) and manganese (II) in water contaminated in coal mining, Quim. Nova 29 (2006) 34–39.
[13] S. Sun, L. Wang, A. Wang, Adsorption properties of cross linked carboxymethyl-chitosan resin with Pb(II) as template ions, J. Hazard. Mater. 136 (2006) 930–937.
[14] E. Birlik, S. Büyüktiryaki, A. Ersöz, A. Denizli, R. Say, Selective separation of thorium using ion imprinted chitosan-phthalate particles via solid phase extraction, Sep. Sci. Technol. 41 (2006) 3109–3121.
[15] U. Ulusoy, S. Simsek, Lead removal by polyacrylamide-bentonite and zeolite composites: effect of phytic acid immobilization, J. Hazard. Mater. 127 (2005) 163–171.
[16] N.N. Greenwood, A. Earnshaw, Chemistry of the Elements, Butterworth-Heinemann Ltd., Cambridge, 1995.
[17] J. Domb, E.G. Cravalho, R. Langer, The synthesis of poly(hydroxamic acid) from poly(acrylamide), J. Polym. Sci. Polym. Chem. 26 (1988) 2623–2630.
[18] T. Laussmann, R. Eujen, C.M. Weisshuhn, U. Thiel, G. Vogel, Structures of diphospho-myo-inositol pentakisphosphate and bisdiphospho-myo inositol tetrakisphosphate from dictyostelium resolved by NMR, Biochem. J. 315 (1996) 715–720.
[19] M.H. Khan, A. Ali, N.N. Khan, Spectrophotometric determination of thorium with disodium salt of Arsenazo-III in perchloric acid, J. Radioanal. Nucl. Chem. 250 (2001) 353–357.
[20] H. Rohwer, N. Rheeder, E. Hosten, Interactions of uranium and thorium with arsenazo III in an aqueous medium, Anal. Chim. Acta 341 (1997) 263–268.
[21] H. Omichi, A. Katakai, T. Sugo, J. Okamoto, A new type of amidoxime-group-containing adsorbent for the recovery of uranium from seawater 3. Recycle use of adsorbent, Sep. Sci. Technol. 21 (1986) 563–574.
[22] R.J. Eldridge, Encyclopedia of Separation Science, Academic Press, 2000.
[23] B.S. Krishna, D.S.R. Murty, B.S. Jai Prakash, Thermodynamics of chromium(VI) anionic species sorption onto surfactant-modified montmorillonite clay, J. Colloid Interface Sci. 229 (2000) 230–236.

[24] A.M. El-Kamash, A.A. Zaki, M. Abed El Geleel, Modeling batch kinetics and thermodynamics of zinc and cadmium ions removal from waste solutions using synthetic zeolite, J. Hazard. Mater. 127 (2005) 211–220.
[25] L. Yun, S. Xing, C. Haidong, Z. Huixian, G. Shixiang, Adsorption of copper and lead in aqueous solution onto bentonite modified by 4′-methylbenzo-15-crown-5, J. Hazard. Mater. 137 (2006) 1149–1155.
[26] S. Sun, A. Wang, Adsorption kinetics of Cu (II) ions using *N*,*O*-carboxymethyl-chitosan, J. Hazard. Mater. 131 (2006) 103–111.
[27] J.C. Miller, J.N. Miller, Statistics for Analytical Chemistry, John Wiley and Sons, New York, 1989.
[28] H.J. van der Maas, Basic Infrared Spectroscopy, Heyden and Son Ltd., London, 1972.
[29] A.R. Cestari, V.F. Eunice, C.R.S. Mottos, Thermodynamics of the Cu(II) adsorption on thin vanillin-modified chitosan membranes, J. Chem. Thermodyn. 38 (2006) 1092–1099.
[30] I. Smiciklas, S. Dimovich, I. Plecas, M. Mitric, Removal of Co^{2+} from aqueous solutions by hydroxyapatite, Water Res. 40 (2006) 2267–2274.